HTML ABSTRACT + LINKS

Transient electric birefringence of wormlike macromolecules in electric fields of arbitrary strength: A computer simulation study

H. E. Pérez Sánchez, J. García de la Torre, and F. G. Díaz Baños[a)]
Departamento de Química Física, Universidad de Murcia, 30071 Murcia, Spain

(Received 19 November 2004; accepted 7 January 2005; published online 25 March 2005)

We have studied the birefringence decay of linear models of macromolecules for two different types of flexibility, the broken-rod chain and the wormlike chain, using a computer simulation of a transient electric birefringence experiment. We have paid particular attention to the influence of the intensity of the orienting field, including two orienting mechanisms, the induced dipole, and the permanent dipole. We have compared wormlike and broken-rod models of the same radius of gyration, finding that they present a different decay curve under the influence of the same intensity of the field. We have seen that these differences are due to the faster relaxation times (smaller in the wormlike chain model) and amplitudes, because, regardless of the type of flexibility, the overall size of a molecule (measured by the radius of gyration) essentially determines the longest relaxation time. We have also analyzed how the relaxation process is affected by the degree of flexibility, the orientation mechanisms, and the intensity of the field. Studying a different aspect, we have paid attention to the deformation of a molecule in a transient electric birefringence experiment as a source of information. In this work we have developed equations to characterize this deformation in terms of one of the components of the gyration tensor, if a dynamic light scattering experiment under the influence of an electric field could be performed. To develop this work we have simulated the Brownian dynamics of the different models, relaxing after the removal of an orienting external electric field of arbitrary strength. A comparison with other methods such a the rigid body treatment or the correlation analysis of Brownian trajectories has also been included. We have seen that differences between the two Brownian dynamics methods are small and that the rigid-body treatment is only an acceptable approximation to obtain the longest relaxation time. © *2005 American Institute of Physics*. [DOI: 10.1063/1.1863892]

I. INTRODUCTION

Transient electric birefringence (TEB), which is based on the time-dependent behavior of a macromolecular solution under the influence of an electric field,[1–3] is well known as an interesting source of information about macromolecules. For example, TEB has been used to characterize the global geometry and flexibility of nucleic acids.[4,5] In such experiments, each system can be characterized from an analysis of the on-field rise or the off-field decay with a set of times and their corresponding amplitudes, although to properly understand the results appropriate models, methods, and theories are needed.

A. Models

For chain macromolecules, such as some helical nucleic acids, it is usually assumed that their flexibility is distributed more or less uniformly along the chain, despite the fact that, sometimes, simple nonhelical structural elements are found in its structure. When modeling flexible macromolecules, the first idea is ideally represented by the wormlike chain model (WLC), while the second can be described by the once-broken-rod chain (BRC). These two extreme models, plus some others, mainly the weakly bending rod and the randomly broken chain have been used to understand TEB experimental results of DNA and RNA (see, for example, Lu *et al.*[6]). It is usual to simplify the models in the form of chains of beads.

B. Orienting mechanisms

One of the basis of a TEB experiment is the mechanism that orients the molecule when an electric field is present. When the orienting mechanism is only based on the interaction of the electric field with a molecular permanent dipole it is accepted as a simple description (see, for example, Frederick and Houssier[1]). But many macromolecules are macroions and in this case the orienting mechanism is complex and not well understood at the present time (see, for example, Grycuk *et al.*[7] and references therein). It is assumed that the induced electric dipole of linear macroions arises from a long range phenomenon which is the distortion of the ion atmosphere from equilibrium by the imposed electric field. In the special case of rigid polylectrolytes this problem has been addressed with relevant contributions through analytical theory (see, for example, Fixman and Jagannathan,[8] Rau and Charney,[9,10] Bellini *et al.*[11]) and simulation procedures.[7] It should be emphasized, however, that the treatment of flexible structures will be even more complex. For flexible models made up of beads connected by virtual bonds, the usual ap-

[a)]Author to whom correspondence should be addressed. Electronic mail: fgb@um.es

 © 2005 American Institute of Physics

Downloaded 05 Apr 2005 to 155.54.98.94. Redistribution subject to AIP license or copyright, see http://jcp.aip.org/jcp/copyright.jsp

proximation is to assume that associated with each virtual bond is an electric polarizability tensor, which is axially symmetric about the bond vector. The molecular electric polarizability tensor is then modeled as the tensor sum over individual virtual bond polarizabilities. This model of orienting mechanism has been named sometimes as "pairwise additive." Lewis *et al.*[12] used this model to developed Brownian dynamics simulations to compare with DNA experimental data. This implies a linear dependence of the molecular polarizability tensor with the molecular weight for nearly rodlike polyions. For DNA, a nearly quadratic dependence on the molecular weight is observed,[13–15] although in one case a cubic dependence has also been observed.[16] Allison and Nambi[17] proposed a simple model which leads to a double-sum formula for the molecular polarizability tensor which has the correct length dependence. This treatment has also been applied to RNA.[18] Heath *et al.*[19] developed an analytical theory for weakly bending rods using the same approach. We have also used this idea to model the induced dipole orienting mechanism in our previous studies.[20–23] As a summary, the orientation mechanism of flexible macroions is complex and the pairwise additive models may be as good as we can do at the present time. The aim of this work is not the study of orientation mechanism of a molecule itself, but we need to be cautious about the results using such models, particularly with addressing questions about macroion flexibility.

C. Analytical theories and Monte Carlo simulation

For wormlike chains (and weakly bending rods), Hearst[24] proposed equations to obtain the longest decay time. Later, Hagerman and Zimm[25] assumed that the longest relaxation time could be adequately predicted as the rigid-body-treatment (RBT) average of the longest of the five relaxation times of wormlike molecules. The same idea is behind the results proposed by García Molina *et al.*[26] for wormlike chains and randomly broken chains. In the RBT, properties are calculated as averages of the values obtained from a set of conformations which are treated as rigid. The appropriate set of conformations is obtained through a Monte Carlo simulation. The hydrodynamic properties of rigid macromolecules can be calculated using well-developed theoretical and computational treatments, using bead models.[27–30] According to this treatment, for a rigid body, the reorientational dynamics involved in processes such as orientation and relaxation under an electric field can be characterized by a set of five rotational relaxation times τ_k, $k=1,\ldots,5$,[31] where τ_1 is the longest time.

For segmentally flexible macromolecules, Wegener and co-workers,[32–35] and Harvey, García de la Torre and co-workers[36–40] developed formalisms to describe their diffusivity, although the degree of flexibility of the joint did not enter into the treatment. Also for these molecules, Roitman and Zimm[41,42] were able to develop a quasianalytical description of the dynamics of the simplest BRC model, the semiflexible trumbbell, for an induced dipole orienting mechanism for the simplified case in which hydrodynamic interaction is neglected and the orientation is produced by very weak fields (Kerr region). Iniesta *et al.*[43] obtained different properties (including τ_1) using the BRC model for a semiflexible once-broken-rod chain. In a different approach, Vacano and Hagerman[44] proposed the τ-ratio method, which has been applied, with certain interesting modifications, to different cases of RNA and DNA.[45–48] The τ-ratio approach is based on the comparison of the longest relaxation times between one linear macromolecule and another with nonhelical elements. This ratio between relaxation times is related with the bond angle through a Monte Carlo simulation. The result is the angle that presents the structure with segmental flexibility. An improved version of this procedure, the "phased τ ratio" has also been proposed.[46]

D. Brownian dynamics simulation

In recent years, it has become common to simulate the Brownian dynamics of macromolecules in solution and their orientation when an electric field is applied, or the related relaxation when this electric field is removed. Two different approaches have been used. Alllison and Nambi[17] studied the electric dichroism and electric birefringence of DNA analyzing the simulated Brownian trajectories (excluding any electric field) using suitable correlation functions. One of the objectives of these authors was to approach the complex nature of polyion alignment in electric fields by comparing two orienting mechanisms, the induced dipole, and the saturated induced dipole. Two correlation functions were proposed (one for each mechanism) and a low-field transient electric birefringence approximation was assumed. This method has been applied in several studies. For example, Zacharias and Hagerman[18] developed an interesting study on the influence of the statical and dynamic bends in the transient electric birefringence of RNA.

On the other hand, our group[20,49–52] studies the changes produced in the birefringence through a direct analysis of the simulated trajectories, including the presence of an electric field. In two previous works[21,22] we investigated the transient electric birefringence of segmentally flexible macromolecules in electric fields of arbitrary strength. In those papers, we studied the decay of the electric birefringence from the steady-state value to zero when an orienting electric field applied on a segmentally flexible macromolecule is switched off.

E. Objectives of this work and preview of the conclusions

The approaches and results summarized above represent important advances for the proper understanding of experimental TEB results. However, our aim is to give an answer to the following questions.

Is the longest relaxation time independent of the type of flexibility of a molecule? The reason to address this issue is that Hearst[24] and, later, Hagerman and Zimm[25] and García Molina *et al.*[26] proposed equations to relate *P*, the persistence length of a wormlike molecule, with the rotational diffusion coefficient and so with τ_1. This treatments implicitly assume that internal motion does not contribute to the longest relaxation time for a wormlike chain. For example,

Downloaded 05 Apr 2005 to 155.54.98.94. Redistribution subject to AIP license or copyright, see http://jcp.aip.org/jcp/copyright.jsp

Hagerman[53] characterized the flexibility of DNA, treated as a wormlike chain, using the result from Hagerman and Zimm.[25] In addition, Diekman *et al.*,[13] for DNA, stated that τ_1 is mainly determined by the averaged conformation. On the other hand, relaxation times are, according to Roitman and Zimm,[42] characteristics of a molecule and, as a consequence, do not depend on the method used to obtain them. Allison and Nambi[17] assumed that the longest lifetime component of electric birefringence (or electric dichroism) corresponds to pure end-over-end rotational diffusion, and proposed that, for a linear model like DNA, the fact that the relaxation times depend on flexibility might simply be due to variations in the end-to-end distance. In the case of a broken-rod chain model, Pérez Sánchez *et al.*[22] concluded that the longest relaxation time depends fundamentally on the overall dimensions of the model. In this work we make a direct comparison of two different flexibility mechanisms (WLC and BRC). We find that, regardless of the type of flexibility, the overall size of a molecule (measured by the radius of gyration) essentially determines the longest relaxation time.

Are there any differences between a wormlike molecule and a broken-rod molecule in a TEB experiment? This question arises because the broken-rod chain and the wormlike chain models have been used frequently to describe the flexibility of macromolecules. One example is the interpretation of experimental data from DNA, usually treated as a WLC,[6] but sometimes as a broken rod.[54] In fact, many real molecules probably present a mixture of both types of flexibility. Good examples are RNA[55] and some cases of DNA.[56] In this work, we find that the WLC and the BRC models present a different decay curve for the same intensity of the field. According to the previous paragraph, the differences must appear in the faster times and in the amplitudes. In fact, the study of faster components has been shown to be important, because they may contribute as much as 80% of the whole decay in molecules with segmental flexibility[21,57,22,18] We find that faster relaxation component is smaller in the WLC model. Regarding amplitudes, we find in this work that the differences in amplitudes between BRC and WLC models are substantial, especially in the induced dipole orienting mechanism.

How is the relaxation process affected by the degree of flexibility, the orientation mechanism, and intensity of the orienting field? This question arises because the dependence of the relaxation on the nature of a given molecule and on the intensity of the field is a source of information that could be exploited. Wegener[33] found that the relative amplitudes (not the time constants) of the decay of birefringence were dependent on the orientation mechanism, particularly, for high curvature angles. We have seen[22] that amplitudes depend on both the intensity of the field and the degree of flexibility for the BRC model. This is consistent with the results obtained by Dieckman *et al.*[13] for DNA, but it is not with the hypothesis of Zacharias and Hagerman[18] for RNA, who affirm that the amplitudes are sensitive to the average and dispersion of the angle but not to the field when working at low fields. In this work we find that in both models amplitudes depend on the orientation mechanism, on the degree of flexibility and on the intensity of the field (usually less in the WLC model and in the induced dipole orienting mechanism). Allison and Nambi[2] proposed two correlation functions for the induced and saturated induced orienting mechanism in the case of quasirigid chains in low electric field, finding, for linear DNA, no significant differences between the molecules simulated with pure induced or saturated induced dipole. We have checked for simple BRC models[21,22] that this two correlation functions give different results for not-straight systems. In this work we find that, for both models, these two functions give different results when the averaged conformation is not straight. Our group has also found that for BRC models[21,22] a distinct behavior for the induced and permanent dipoles in the relaxation process. In this work we find that, in the WLC model, differences in the decay profile are significant between orienting mechanisms and field intensity, at high flexibility values. Regarding the time spectrum, Allison and Nambi[17] suggested that lifetimes are insensitive to field strength. Our group showed that, for BRC models[21,22] the time spectrum has no dependence on the type of dipole or the field intensity. In this work we extend the limits of flexibility and field intensity of previous works and increase the detail of our previous BRC model for the comparison of the WLC and BRC models. Our results show that the main dependence of the faster relaxation times is the type of flexibility, the dependence on the orienting mechanism is detectable and for the permanent dipole a certain dependence on the field intensity is also detectable.

What information can be obtained from the deformation of a molecule under the influence of an electric field? We have addressed this question because in a TEB experiment, a flexible molecule is deformed by an electric field of any intensity.[22,23] Of course, the magnitude of such deformation is directly related with the orienting mechanism, the intensity of the field and the type and degree of flexibility. Allison and Nambi[17] and Zacharias and Hagerman[18] assumed the existence of the "low field" criterion, whereby the lack of deformation of the molecule should lead to the independence of the obtained results with respect to the intensity of the field. However, according to our previous studies,[21,22] the relaxation for the induced dipole could be the same for low and high fields, while for the permanent dipole, it could depend on the intensity of the field even at low fields. For a non-straight BRC model Pérez Sánchez *et al.*[22] found that, for permanent dipoles, the effect of deformation on the decay profile is slight in most cases and even less significant for the slower components, while for induced dipoles, on average, no deformation is observed for any field intensity or any degree of flexibility. In this work we develop equations which show how the deformation of a molecule could be followed and interpreted in terms of one of the components of the gyration tensor if, what we call a dynamic electric field light scattering experiment (DEFLS), could be performed. This technique should be a dynamic light scattering experiment for a macromolecular solution which is (or has been) under the influence of an electric field. We also include in this work simulation results for these possible experiments, and an analysis of what information could be obtained from them. We find that the longest relaxation times for the relaxation of the measurable component of the gyration tensor are

Downloaded 05 Apr 2005 to 155.54.98.94. Redistribution subject to AIP license or copyright, see http://jcp.aip.org/jcp/copyright.jsp

slightly higher than those of birefringence. We also find that there is less deformation and faster recovery in the WLC model under the influence of the same field for the permanent dipole orienting mechanism.

Which are the differences in the results obtained from the rigid body treatment and the two Brownian dynamics methods mentioned above? This is a methodological question suggested by the following facts. As we mentioned above Hagerman and Zimm[25] assumed that the longest relaxation time could be adequately predicted as the rigid-body-treatment average of the longest of the five relaxation times of wormlike molecules. The same idea is behind the results proposed by García Molina *et al.*[26] for wormlike chains and randomly broken chains. In the case of a BRC model, Pérez Sánchez *et al.*[22] compared their results with those offered by the hydrodynamic theory[30] and Wegener[33] for rigid models, finding that the RBT appears to provide a reasonable approximation when the quality of the data is not critical. In this work our results show that the values obtained with the RBT for τ_1 are usually very close to those obtained from Brownian dynamics simulation but the values of the faster relaxation times are totally different for RBT and Brownian dynamics simulation. A different point is that the correlation functions proposed by Alllison and Nambi[2] for rather rigid DNA fragments have been used by Zacharias and Hagerman[74] to study models of high segmental flexibility. Our results show that differences in the decay curves between the direct analysis of the simulated trajectories, including the presence of an electric field and the analysis with correlation functions are small, what suggests that correlation analysis could be usable in both models of flexibility.

II. MODELS AND METHODS

A. Models: Broken rod chain and wormlike chain

We consider two different models of macromolecular chains, both made up of $N+1=11$ elements: a segmentally flexible macromolecule composed of two quasirigid arms joined by a semiflexible swivel (BRC) and a macromolecule with its flexibility equally distributed along the chain (WLC). The mechanical, hydrodynamic, and electro-optical description of the model is as described in earlier papers.[20,21,25,23] Here, we summarize a few essential features.

The potential energy of a given configuration of the model has two contributions, V_{int} and V_{elect}. V_{int} has two contributions $V_{int,s}$ and $V_{int,b}$, the first due to the stretching of the Hookean springs connecting each pair of consecutive beads. These springs are defined as quasirigid with a spring constant such that their rms elongation is $\langle b^2\rangle = 1.05 b_0^2$, i.e., only 5% longer than their square equilibrium length b_0.[58] The second contribution, is the term associated to the bending, $V_{int,b}$, which is defined by

$$\frac{V_{int,b}}{k_B T} = \sum_{i=1}^{N-1} Q_i(\alpha_i - \alpha_{0,i})^2. \tag{1}$$

In Eq. (1), $\alpha_{0,i}$ is the equilibrium value of the angle defined by two consecutive subunit axes ($\alpha_{0,i}=0$ for fully extended, straight conformation) and Q_i is the flexibility parameter,

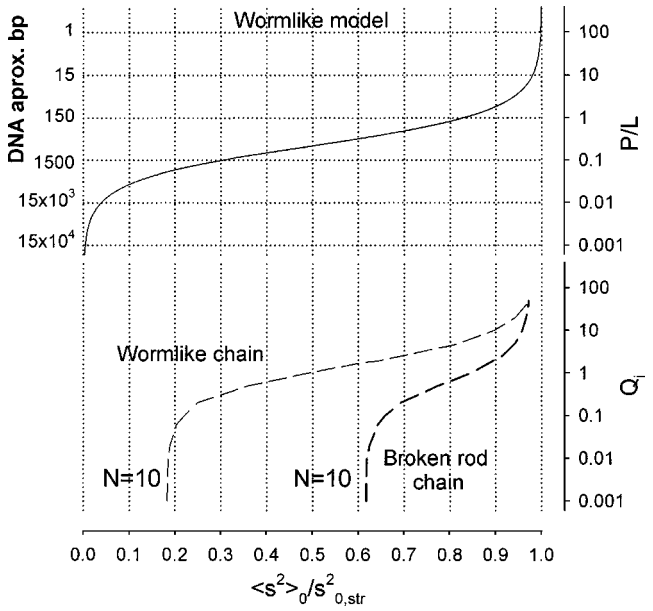

FIG. 1. Relation between three different ways of characterizing flexibility (P/L, Q, and $\langle s^2\rangle_0/s^2_{0,str}$) for a wormlike model, a wormlike chain, and a broken-rod chain. Results obtained with $\alpha_0=0$. The plot for the wormlike model was obtained from Eq. (2). For wormlike and broken-rod chains the computational result obtained from Monte Carlo simulation are presented. For differences in the values of Q_i for wormlike and broken-rod chains see text. For illustrative purposes, the approximate correspondence between the number of base pairs of DNA with $P=50$ nm and P/L is included.

with $Q_i=0$ for the completely flexible case and $Q_i=50$ for the quasirigid case. The combination of different values of $\alpha_{0,i}$ and Q_i define our model. For example, in the BRC all $Q_i=50$, except that corresponding to the central hinge, which will depend on the flexibility that we shall try to reproduce. In the WLC all Q_i will be the same and the value will depend once again on the flexibility of the model (see Fig. 1).

As regards the modeling of wormlike flexibility, we remind the reader that the mean of the squared radius of gyration of an infinitely thin macromolecule is given by[59]

$$\langle s^2\rangle_0 = \frac{LP}{3} - P^2 + \frac{2P^3}{L}\left[1 - \frac{P}{L}(1 - e^{L/P})\right]. \tag{2}$$

In Eq. (2), P is the persistence length and L is the contour length. The subscript zero indicates the absence of any external deforming agent. In this case $s^2_{0,str}=L^2/12$, with $s^2_{0,str}$ being the squared radius of gyration for a rigid straight molecule. As argued in a previous work,[23] there are different ways of defining the flexibility of a wormlike molecule. One of these is P/L (P should not be the only parameter used), while another is to use $\langle s^2\rangle_0/s^2_{0,str}$. This way of presenting flexibility is very convenient because it has the advantage of being independent of the model (type of flexibility and number of subunits). When using linear chain models of several subunits, flexibility is discretely localized in the hinges of the chain. Flexibility in these chain models is defined by parameters Q_j. In Fig. 1 we present plots to illustrate the relation between these three different ways of characterizing flexibility. A discussion of these types of figures can be read in Ref. 23.

In this paper, we study the WLC model and, for com-

Downloaded 05 Apr 2005 to 155.54.98.94. Redistribution subject to AIP license or copyright, see http://jcp.aip.org/jcp/copyright.jsp

parison, the BRC model. We have found that $N=10$ is a suitable number of subunits to represent wormlike flexibility within a wide range of P/L values. At the same time, $N=10$ is a reasonable compromise between the degree of detail given by the model and the computational time required.

For properties which only depend on the overall dimensions, we find the representation proposed in Fig. 1 to be very useful. First, there is a region in which the overall dimensions of a given macromolecule can be described computationally by both WLC and BRC. In addition, this allows us to choose the most suitable model to represent, for example, DNA, because the expected values of P/L for DNA molecules of different lengths can be readily obtained. For illustrative purposes, Fig. 1 contains an axis with the approximate number of base pairs (bp) corresponding to some values of P/L (it is assumed that $P=50$ nm with a rise per base pair of 0.34 nm). For instance, a DNA of ≈ 150 bp could be represented as a wormlike chain with $N=10$ segments and $Q_j \approx 8$. The same molecule could also be represented by a broken rod of $N=10$ and a central hinge with $Q_j \approx 1$.

B. Brownian dynamics simulation

The Brownian dynamics simulation of semiflexible macromolecules has been used previously by our group.[58,60–64] We use a simulation procedure based on Ermak and McCammon's algorithm,[65] with a modification proposed by Iniesta and García de la Torre.[66] Each step is taken twice, in a predictor-corrector manner, and the position of the beads after the time step are obtained from the previous ones. When the hydrodynamic interaction (HI) between beads is included we use the Rotne–Prager–Yamakawa modification of the Oseen tensor,[67,68] which corrects for the nonpointlike nature of the frictional elements and correctly describes the possibility of overlapping (for equal-sized beads).

C. Brownian dynamics with electric field

Interaction between the molecule and the field is due to permanent or induced dipoles. The corresponding potential energy is given by

$$\frac{V_{elect}}{k_B T} = -\sum_{i=1}^{N} (a_i \cos\theta_i + b_i \cos^2\theta_i), \tag{3}$$

where $\cos\theta_i = (\mathbf{E}\cdot\mathbf{u}_i)/E$ is the cosine of the angle between the electric field E, and the arm vector $\mathbf{u}_i$.

The parameters that describe the intensity of the molecule-field interaction are

$$a_i = \frac{\mu_i E}{k_B T}, \tag{4}$$

$$b_i = \frac{(\epsilon_i^{\parallel} - \epsilon_i^{\perp})E^2}{2k_B T}. \tag{5}$$

The electric parameters are $a_i=0$ for a purely induced moment and $b_i=0$ for a purely permanent dipole moment. In the case of permanent dipoles, we shall consider one possibility: the head-to-tail case, in which a_i is negative ($\boldsymbol{\mu}_i$ is in the opposite direction to $\mathbf{u}_i$) and which is relevant for both BRC and WLC. The field intensity, or more precisely, the strength of the molecule-field interaction is governed by the values of the $a's$ and $b's$, a being proportional to E and b proportional to E^2.

In the present study we deal exclusively with the birefringence decay. Therefore, the field-on, birefringence-rise first part of the simulation, which has to be long to make sure that the steady state is reached, is somehow useless for our purposes. In order to save computing time, we start the simulation with a sample of molecules generated with the Monte Carlo procedure in the presence of field. We add a period of time for the system to stabilize using the Brownian dynamics procedure. At this point, the field is removed. For the birefringence decay, we use the Brownian dynamics algorithm and individual trajectories are simulated for a large number of molecules. At any given time, t, $P_2(\cos\theta_i)$ is evaluated for each arm ($i=1,2$), with P_2 being the Legendre polynomial of degree 2, defined by $P_2(\cos\theta_i)=(3\cos^2\theta_i-1)/2$. For each molecule, birefringence is calculated following

$$\Delta n(t) = \frac{1}{\sum_{i=1}^{N} b_{i(i+1)}} \sum_{i=1}^{N} b_{i(i+1)} P_2(\cos\theta_i). \tag{6}$$

Equation (6) is a weighted sum in which b_i is the instantaneous connector (spring) length. For practical purposes, in our models we can approach every pre-P_2 term equal to $1/N$. The sample averages, and, later, the final values are obtained from Eq. (6). The duration of the decay is sufficiently long for the final birefringence to be zero within statistical error. In this way, when the field is ∞, then $\Delta n(t)=1$.

A way of expressing the results is to normalize to the zero-time value, defining $t=0$ when the field is switched-off,

$$\Delta n(t)^* = \frac{\Delta n(t)}{\Delta n(0)}. \tag{7}$$

Unless we state otherwise, we shall use the normalization given by Eq. (7).

For a more detailed description of the Brownian dynamics with electric field (BDEF) method (including Monte Carlo simulation), the reader is referred to our previous papers.[21,22]

In the same way that Eq. (7) gives a normalized value for birefrigence, it is useful to use dimensionless variables and parameters in both the simulation procedure and for the presentation of the results. Therefore, lengths and distances are expressed in dimensionless form by dividing them by the spring length b; forces are divided by $k_B T/b$ and time is normalized by multiplying by $kT/\zeta b^2$, where $\zeta = 6\pi\eta_0\sigma$, with η_0 being the solvent viscosity and σ the bead radius. To make the field parameters independent of the number of subunits used to model a given macromolecule, the field strength must be expressed as $a^* = a \times N$ and $b^* = b \times N$. An asterisk hereafter denotes all dimensionless quantities.

D. Brownian dynamics simulation without electric field

The correlation analysis of the Brownian dynamics simulation of macromolecules allowed us to obtain different

Downloaded 05 Apr 2005 to 155.54.98.94. Redistribution subject to AIP license or copyright, see http://jcp.aip.org/jcp/copyright.jsp

parameters. In this particular case, Allison and Nambi[17] proposed correlation functions that characterize the rotational dynamics. The procedure is as follows.

We define a unitary vector **A** fixed to a coordinate system that moves with the particle. If $\theta_{\mathbf{A}}$ is the angle formed between two orientations of this vector separated by a time t, then we can define $\cos\theta_{\mathbf{A}}(t)=\mathbf{A}(t)\cdot\mathbf{A}(0)$. The correlation functions of interest are defined as $F(0,t)=f[P_i(\cos\theta_{\mathbf{A}})]$, where P_i is the Legendre polynomial of degree i; more specifically $P_1[\cos\theta_{\mathbf{A}}(t)]=\cos\theta_{\mathbf{A}}(t)$ and P_2 is as defined above.

The functions proposed by Allison and Nambi[17] are

$$H_s(lt',mt')=\frac{1}{N^2}\sum_{ik}P_2[\cos(\mathbf{u}_i(mt')\cdot\mathbf{u}_k(lt'))], \tag{8}$$

$$H_i(lt',mt')=\frac{1}{N^3}\sum_{ik}P_1[\cos(\mathbf{u}_i(mt')\cdot\mathbf{u}_j(mt'))]\times P_2[\cos(\mathbf{u}_j(mt')\cdot\mathbf{u}_k(lt'))]. \tag{9}$$

According to the authors, the first corresponds to an induced dipole and the second to a saturated induced dipole. From now on, we shall name them CF1 and CF2, respectively.

E. Birefringence decay functions and fittings

In principle, one can assume that the dynamics is governed by a series of relaxation times τ_k, so that the normalized birefringence decay would be a series of exponential terms

$$\Delta n(t)^*=y(t)=a_1e^{-t/\tau_1}+a_2e^{-t/\tau_2}+\cdots. \tag{10}$$

Due to normalization, the $y(t)$ functions decay from $y(0)=1$ to $y(\infty)=0$, so that, in this case, $a_1+a_2+\cdots=1$.

When this is reduced to a double exponential, we can write

$$\Delta n(t)^*=y(t)=a_1e^{-t/\tau_1}+(1-a_1)e^{-t/\tau_b}. \tag{11}$$

In Eq. (11), the longest relaxation time and its amplitude are maintained. The term $(1-a_1)$ contains the amplitudes of all the faster modes, $(1-a_1)=a_2+a_3+\cdots$, while τ_b, which could be called the internal relaxation time, is some mean relaxation time that represent the average of the second and following τ's.

Simulations of Brownian dynamics simulation without electric field (BDCF) have been performed using our BD simulation programs.[69] For the multiexponential fit, we have used the commercial program SIGMAPLOT.[70]

F. Rigid body treatment

As mentioned above, although a complete theory of the dynamics of flexible macromolecules cannot be worked out, some approximations or assumptions permit the theoretical description of certain aspects.

The rigid-body treatment (RBT) is fully implemented in the computer program HYDRO[30] for structures of N spheres. Once the coordinates and sizes of the spherical elements have been defined, including relaxation times, a variety of data can be obtained immediately.

It is interesting to compare the values obtained for rigid and flexible models. The values of a rigid equivalent to a flexible structure for BRC are easy to obtain because the only parameter in this case is the averaged value of the central angle. When we try to apply the RBT to finding the rigid equivalent for a WLC model the situation is much more complex, because the number of parameters is much higher. There are different approximations, but among them we have chosen the following: we generate a high number of conformations with the same overall dimensions, measured by s^2, as the value of $\langle s^2\rangle$ for the WLC model. For each of the generated conformations, we calculate their relaxation times and the final value is obtained as an average. The results shown in this work were obtained in this way.

G. Relaxation of the deformation produced by the field

One of the consequences of the action of the field is that the molecule is deformed and its averaged dimensions are modified. The change in the radius of gyration may be expressed in terms of a deformation ratio[71] as the change in $\langle s^2\rangle$ relative to its unperturbed value. This definition can be extended to all the diagonal components of the gyration tensor. In previous works[20,23] we developed these expressions to obtain the deformation of a molecule in a steady-state birefringence experiment under the influence of the field and it is straightforward to extend these results to a transient experiment. In this case, the gyration tensor and, as a consequence, the deformation are functions of time, and the unperturbed value of the radius of gyration is obtained at the limit, $t=\infty$. Hence, the deformation ratio δ^2 can be written as

$$\delta(t)^2=\frac{\langle s(t)^2\rangle-\langle s(\infty)^2\rangle}{\langle s(\infty)^2\rangle}. \tag{12}$$

We can extend this definition to all diagonal components of the gyration tensor

$$\delta(t)^2_{\alpha\alpha}=\frac{\langle G(t)\rangle_{\alpha\alpha}-\frac{1}{3}\langle s(\infty)^2\rangle}{\frac{1}{3}\langle s(\infty)^2\rangle}. \tag{13}$$

From Eqs. (12) and (13) it follows that

$$\delta(t)^2=\tfrac{1}{3}(\delta(t)^2_{xx}+\delta(t)^2_{yy}+\delta(t)^2_{zz}). \tag{14}$$

Following the equations obtained by Pérez Sánchez *et al.*[23] for steady-state birefringence, the deformation of a model, based on equal axially symmetric subunits, in a TEB experiment, can be written as

$$\delta(t)^2_{xx}=\frac{\delta(t)'^2_{xx}\langle s(\infty)'^2\rangle+\Delta n(t)(G^\perp-G^\parallel)}{\langle s(\infty)'^2\rangle+(2G^\perp+G^\parallel)}, \tag{15}$$

$$\delta(t)^2_{zz}=\frac{\delta(t)'^2_{zz}\langle s(\infty)'^2\rangle-2\Delta n(t)(G^\perp-G^\parallel)}{\langle s(\infty)'^2\rangle+(2G^\perp+G^\parallel)}, \tag{16}$$

$$\delta(t)^2=\frac{\delta(t)'^2\langle s(\infty)'^2\rangle}{\langle s(\infty)'^2\rangle+(2G^\perp+G^\parallel)}. \tag{17}$$

In Eqs. (15)–(17) the primed values are those obtained for a model in which the subunits were replaced by pointlike ele-

Downloaded 05 Apr 2005 to 155.54.98.94. Redistribution subject to AIP license or copyright, see http://jcp.aip.org/jcp/copyright.jsp

ments with masses m_i positioned at the center of the subunit, while $G^{\perp}$ and $G^{\parallel}$ are the perpendicular and parallel components of the gyration tensor of each subunit.

One particular situation of interest is when all the subunits are spherical. Then, the subunit gyration tensor is isotropic and the diagonal components are all equal to $\sigma^2/5$, one third of the radius of gyration of one sphere or radius σ. In this case, Eqs. (15)–(17) become, respectively,

$$\delta(t)_{xx}^2 = \frac{\delta(t)_{xx}'^2 \langle s(\infty)'^2 \rangle}{\langle s(\infty)^2 \rangle}, \tag{18}$$

$$\delta(t)_{zz}^2 = \frac{\delta(t)_{zz}'^2 \langle s(\infty)'^2 \rangle}{\langle s(\infty)^2 \rangle}, \tag{19}$$

$$\delta(t)^2 = \frac{\delta(t)'^2 \langle s(\infty)'^2 \rangle}{\langle s(\infty)^2 \rangle}. \tag{20}$$

When N is high, the radius of gyration of one sphere is small compared with the radius of gyration of the whole model, and so $\langle s(\infty)^2 \rangle \approx \langle s(\infty)'^2 \rangle$ and, as a consequence $\delta(t)_{xx}^2 \approx \delta(t)_{xx}'^2$, $\delta(t)_{zz}^2 \approx \delta(t)_{zz}'^2$, and $\delta(t)^2 \approx \delta(t)'^2$.

The average size of a macromolecule, as determined by the radius of gyration, is often obtained from the low angle scattering of light or another type of electromagnetic radiation. When the macromolecule is deformed in an electric field, it may be possible to obtain some components of the gyration tensor from scattering with various geometries. Instrumental and theoretical aspects of the technique of electric field light scattering have been described in the literature.[72,73] The dependence of scattered intensity on the scattering direction is represented by the scattering form factor $P(\mathbf{q})$, with $\mathbf{q}$ being the scattering vector with modulus $q=(4\pi/\lambda)-\sin(\theta_s/2)$, where λ is the radiation wavelength and θ_s is the angle subtended by the scattering direction and the prolongation of the incident beam. For low-angle scattering, we can write[50]

$$P(\mathbf{q}) = 1 - \mathbf{q}^T \langle \mathbf{G} \rangle \mathbf{q}. \tag{21}$$

A particular situation of interest is that corresponding to an experimental setup in which scattering is observed in the (x,y) plane of the lab-fixed system of coordinates, with x being the direction of the incident beam and the external agent acting along the z direction. In this case, we can assume that this agent produces a distribution of mass with cylindrical symmetry around the main direction. Then

$$P(\mathbf{q}) \approx 1 - q^2 \langle G \rangle_{xx}. \tag{22}$$

Equation (22) has been obtained for steady-state light scattering. If we perform experiments following the relaxation of the molecule, it is straightforward to obtain the change of the scattering form factor as a function of time

$$\frac{P(q,\infty) - P(q,t)}{1 - P(q,\infty)} \approx \frac{\langle G(t) \rangle_{xx} - \langle G(\infty) \rangle_{xx}}{\langle G(\infty) \rangle_{xx}} = \delta(t)_{xx}^2. \tag{23}$$

This experimentally feasible combination yields the change in the component of $\langle \mathbf{G} \rangle$, which is independent of the scattering angle.

According to the previous equations, once the field is removed, the deformation produced in a TEB experiment relaxes following a certain time course. Experiments of dynamic electric field light scattering might be able to measure this evolution.

III. RESULTS AND DISCUSSION

We have studied the relaxation process of Δn, paying attention to both the influence of the intensity of the orienting field for broken-rod chains and wormlike chains. In both models the equilibrium angles are 0°. In addition, deformation was studied, including the time evolution after removing the field of δ_{xx}^2, δ_{zz}^2, and δ^2.

A. Birefringence

Our study is devoted to a comparison of the results of the TEB decays (amplitudes and relaxation times) obtained from two models, the BRC and the WLC (both with $\alpha_{0,i}=0$). For the BRC model, this is an extension of the study presented in a previous paper, changing the model from $N+1=3$ to $N+1=11$ elements[22] and allows us to compare BDEF with BDCF and with analytical methods for rigid models (RBT).

In the BDEF, we simulated the birefringence decay for different cases of the field strength for both the induced and permanent dipole orienting mechanisms, including the extreme value of infinitely high. The study of birefringence dynamics at very high (saturating) fields is uncommon in experimental work because of the problems associated with instrumentation, sample alterations, and data interpretation, but for our purposes this extreme situation is very illustrative. The rest of the values were included so that the field strength effects could be studied. The lower limit in the range of field strength is established by the compromise between the statistical quality of the data obtained from our simulations and a reasonable computing time.

In these Brownian dynamics simulations, the time step was $\Delta t^* = 5 \times 10^{-4}$. To analyze the birefringence decay, the system has to reach steady-state birefringence as the starting $(t=0)$ point. As mentioned before, we included a stabilization period, simulated with the Brownian dynamics algorithm of 10–15 units of time. Later we removed the electric field and allowed the system to relax. In order to be certain that the molecules had enough time to relax completely, the duration of each trajectory was between 50 and 100 units of dimensionless time.

In the BDCF, obviously, one decay profile was obtained for each model and orientation mechanism. In these simulations, the time step was also $\Delta t^* = 5 \times 10^{-4}$. The correlation analysis was extended up to $t^* = 100$. Every simulation had a length of 2×10^7 steps and was divided into 16 subsets.

The difficulties of fitting experimental or simulation results to multiexponential curves are well known. To diminish these problems the statistics must be of good quality. We found that to obtain good fittings of the decay data the number of molecules needs to be very high, the reasons being the same as those we mentioned in previous studies.[21,22] In this case, we found that four independent simulations of 50 000

Downloaded 05 Apr 2005 to 155.54.98.94. Redistribution subject to AIP license or copyright, see http://jcp.aip.org/jcp/copyright.jsp

molecules for the best conditions (low flexibility and high fields) and four independent simulations of 200 000 for the worst (high flexibility and low field) are reasonable choices. We have taken special care to obtain reproducible results using the following procedure. Amplitudes and relaxation times are obtained from each of the four simulation sets of data with and without the possibility of a base line (the first check is that the base line must be very close to 0). Later, we obtained another set of data which is the average of the four other simulation sets. This new "global" set is also submitted to the same fitting procedure. Finally, we have four groups of amplitudes and relaxation times. Only when these four groups are nearly identical we can say that the necessary reproducibility has been reached. Of these four sets of fitting results, in this paper we show the one which is the average of the four individual results without base line. In this way, we can include a value of the standard deviation of each parameter.

Following Eq. (11), our decay results were submitted to biexponential analysis, obtaining the amplitudes and relaxation constants. In most of the curves, a third exponential can be detected accurately, but we think it is more illustrative for our purposes to present these results in the same format. In addition, and given the statistical quality of the data, other authors have used biexponential fittings, which are usually the form in which experimental results are presented. Finally, there is the advantage that biexponential fitting is more robust than a triexponential fitting and, in the cases studied, the improvement offered by a third exponential is not dramatic. Note that in the decay from very high fields obtained in BDEF, birefringence is initially saturated, so that $\Delta n(0)^*=1$. In the rest of the cases, the values have been normalized to that at $t=0$. In BDCF, the values are normalized in a way that $\Delta n(0)^*=1$.

All the results mentioned above are presented in Tables I and II. Although we have made the calculations, these tables do not include the values of the quasirigid structure $[\langle s(\infty)^2\rangle/s_{str}^2=0.97]$, because, in all cases, a monoexponential decay with the same $\tau_1^*=18.8$ is obtained.

The tables in this paper have been organized according to the value of $\langle s(\infty)^2\rangle/s_{str}^2$, which, as explained above is a measure of the flexibility that allows comparison between different models. Table I shows results for two different orienting mechanisms of models with $\langle s(\infty)^2\rangle/s_{str}^2=0.62$. In order to illustrate the influence of small changes in the overall dimensions on the relaxation results, Table II shows the results of the two models but with slightly different values of $\langle s(\infty)^2\rangle/s_{str}^2$, namely, 0.77 and 0.79.

Although it is not the aim of this work to study the effect of hydrodynamic interaction (HI), a few simulations including this effect were performed, modeling each of the 11 elements as a sphere with a radius of 0.5. The values of the relaxation times obtained with HI are significatively smaller (especially for the longest time) and the amplitudes are practically the same although, in principle, the same general conclusions are reached. Simulations without HI are computationally much shorter and, given that our objective is not comparison with given experimental data (in this case HI should be included), we have preferred to develop our study without including hydrodynamic effects.

B. Dynamic electric field light scattering

An electric field has the effect of deforming the molecule, and this aspect has also been treated. This deformation is manifested in a change of the diagonal components of the gyration tensor, which will vary depending on the field strength, flexibility, and the orienting mechanism. As we have shown above, the dynamic electric field light scattering (DEFLS) technique should be able to follow these changes as a function of time for the *xx* component.

We have studied δ_{xx}^2, which is a combination of orientation and deformation effects. From its evolution with time after removal of the electric field, a clear multiexponential fitting procedure is suggested (see, for example, Fig. 2). As a consequence we have followed the same procedure as described above for fitting the birefringence decay data. It should be mentioned that the statistical quality of the $\delta(t)_{xx}^2$ data is slightly better than the corresponding birefringence results.

All the results are presented in Tables I and II.

C. Discussion of the results

In accordance with our objectives, we demonstrate that our methodology is able to yield results for the amplitudes and relaxation times that characterize a TEB relaxation decay for molecules with a different degree of flexibility under electric fields of arbitrary strength (Figs. 3 and 4 and Tables I and II). We also show some results for the time dependence of deformation in the simulated TEB experiments.

Our results show that, regardless of the type of flexibility, the overall size (measured by the radius of gyration) essentially determines the longest relaxation time. As a consequence, it is the response to the electric field and the whole off-field relaxation curve that should mark differences between different models, and these differences should be reflected in the rest of the relaxation times and amplitudes. This fact widens the interest of birefringence experiments. In addition, this conclusion agrees with the proposed idea[17,13,74,53,25,22] that τ_1 depends on the end-over-end rotation, but adds a quantitative relationship for the experimentally obtained radius of gyration. On the other hand, τ_1 has been used to characterize the flexibility of a molecule (see, for example, some recent Refs. 6 and 56), and this fact enlarges the interest of the comparison of these two different models. As a consequence, we have organized Tables I and II according to the values of the radius of gyration in the absence of the field ($t=\infty$). In Table II small differences in τ_1 appear between the BRC and WLC models, the main reason being the small difference in $\langle s(\infty)^2\rangle/s_{str}^2$.

The WLC model and the BRC model present a different decay curve for the same intensity of the field. These differences are detectable both with the induced dipole orienting mechanism and with the permanent dipole orienting mechanism. In Figs. 2 and 3, two models with the same $\langle s(\infty)^2\rangle/s_{str}^2$ are compared. As can be expected (see previous paragraph),

Downloaded 05 Apr 2005 to 155.54.98.94. Redistribution subject to AIP license or copyright, see http://jcp.aip.org/jcp/copyright.jsp

TABLE I. (a) Fitting results of the decay profiles of birefringence and deformation obtained with Brownian dynamics simulation with electric field for models with the same $\langle s(\infty)^2\rangle/s_{str}^2=0.62$. Models with N+1=11 elements. Equilibrium conformation. Straight ($\alpha_{0,i}=0$). Simulations performed without hydrodynamic interaction. Permanent dipole orienting mechanism. For references and procedures to obtain these data, see text. (b) As (a), but for induced dipole orienting mechanism. Values obtained for rigid models with the same s^2/s_{str}^2 are also included. These results are obtained with the RBT and they do not depend on the type of orienting mechanism.

	Model	Field	$\Delta n(0)^*$	a_1	τ_1^*	τ_b^*
(a)						
	BRC	$a^*=\infty$	1.000±0.000	0.63±0.02	9.5±0.2	2.6±0.2
		$a^*=10$	0.505±0.001	0.72±0.04	9.7±0.3	2.9±0.3
		$a^*=5$	0.256±0.001	0.73±0.06	10.2±0.4	3.4±0.5
		$a^*=2.5$	0.079±0.000	0.77±0.14	10.4±1.0	3.5±1.4
		CF2	⋯	0.56±0.01	9.6±0.1	3.1±0.1
$\Delta n(t)^*$						
	WLC	$a^*=\infty$	1.000±0.000	0.50±0.00	9.2±0.1	0.57±0.02
		$a^*=10$	0.362±0.002	0.76±0.00	9.8±0.1	0.95±0.02
		$a^*=5$	0.195±0.001	0.83±0.02	10.0±0.2	1.1±0.3
		$a^*=2.5$	0.064±0.001	0.82±0.10	10.3±0.9	2.3±1.9
		CF2	⋯	0.76±0.01	9.9±0.1	0.93±0.03
			$-\delta(0)_{xx}^2$			
	BRC	$a^*=\infty$	0.992±0.001	0.95±0.54	9.4±5.0	
		$a^*=10$	0.513±0.001	0.97±0.00	10.2±0.1	
		$a^*=5$	0.259±0.001	0.98±0.01	10.7±0.3	
		$a^*=2.5$	0.087±0.001	0.95±0.01	12.1±0.3	
$-\delta(t)_{xx}^2$						
	WLC	$a^*=\infty$	0.991±0.001	0.93±0.54	10.2±5.3	
		$a^*=10$	0.535±0.002	1.02±0.01	10.8±0.3	
		$a^*=5$	0.299±0.001	1.04±0.01	10.8±0.3	
		$a^*=2.5$	0.102±0.001	1.05±0.03	11.0±0.3	
(b)						
	BRC	$b^*=10$	0.621±0.001	0.25±0.02	9.9±0.4	3.8±0.1
		$b^*=5$	0.356±0.001	0.29±0.01	9.3±0.2	3.6±0.4
		$b^*=2.5$	0.176±0.000	0.35±0.09	9.1±1.4	3.5±0.2
		CF1	⋯	0.31±0.02	9.6±0.3	3.6±0.1
		RBT	⋯	⋯	10.7	7.07
$\Delta n(t)^*$						
	WLC	$b^*=10$	0.351±0.001	0.66±0.01	9.6±0.1	0.77±0.03
		$b^*=5$	0.175±0.001	0.66±0.01	9.7±0.1	0.77±0.01
		$b^*=2.5$	0.083±0.001	0.64±0.03	9.7±0.5	0.95±0.19
		CF1	⋯	0.65±0.01	9.6±0.1	0.95±0.02
		RBT	⋯	⋯	10.2±0.3	6.2±0.6
			$-\delta(0)_{xx}^2$			
	BRC	$b^*=10$	0.636±0.001	0.54±0.07	11.0±0.7	4.6±0.4
		$b^*=5$	0.365±0.001	0.58±0.04	10.7±0.3	4.1±0.3
		$b^*=2.5$	0.183±0.001	0.47±0.20	12.1±2.6	4.4±1.4
$-\delta(t)_{xx}^2$						
	WLC	$b^*=10$	0.509±0.001	0.96±0.01	10.1±0.1	
		$b^*=5$	0.269±0.001	0.95±0.01	9.5±0.3	
		$b^*=2.5$	0.130±0.001	0.95±0.01	9.1±0.4	

in all cases the differences are concentrated in the first part of the decay, with a relaxation for the WLC model faster in the first part of the decay than that of the BRC model.

Differences in amplitudes between the WLC and BRC models are substantial, especially in the induced dipole orienting mechanism. We have seen previously[21,22] that for the BRC model, amplitudes depend on the orienting mechanism, the intensity of the field and the flexibility of the model, which is clearly confirmed by the results presented in this work. The differences between the induced and permanent dipole orienting mechanisms are higher in the BRC. From these findings amplitudes could be useful for distinguishing between wormlike and segmental flexibility.

τ_b is smaller in the WLC model. Numerically, this is clear from Tables I and II, and is more evident when $\langle s(\infty)^2\rangle/s_{str}^2$ is greater. For example, the τ_b of the more flex-

Downloaded 05 Apr 2005 to 155.54.98.94. Redistribution subject to AIP license or copyright, see http://jcp.aip.org/jcp/copyright.jsp

TABLE II. Fitting results of the decay profiles of birefringence and deformation obtained with Brownian dynamics simulation with electric field for models with slightly different values of the average radius of gyration. For BRC, $\langle s(\infty)^2\rangle/s_{str}^2=0.77$. for WLC, $\langle s(\infty)^2\rangle/s_{str}^2=0.79$. Models with $N+1=11$ elements. Equilibrium conformation: straight ($\alpha_{0,i}=0$). Simulations performed without hydrodynamic interaction. Permanent dipole orienting mechanism. For references and procedures to obtain these data, see text. (b) As (a), but for induced dipole mechanism. Values obtained for rigid models with the same s^2/s_{str}^2 are also included. These results are obtained with the RBT and they do not depend on the type of orienting mechanism.

	Model	Field	$\Delta n(0)^*$	μ_1	τ_1^*	τ_b^*
(a)						
$\Delta n(t)^*$	BRC	$a^*=\infty$	1.000±0.000	0.69±0.01	13.2±0.1	2.0±0.1
		$a^*=10$	0.556±0.000	0.81±0.01	13.3±0.1	2.2±0.2
		$a^*=5$	0.338±0.001	0.86±0.02	13.3±0.3	2.5±0.4
		$a^*=2.5$	0.164±0.002	0.88±0.05	13.8±0.7	3.2±1.9
		CF2	⋯	0.78±0.01	12.8±0.0	2.2±0.0
	WLC	$a^*=\infty$	1.000±0.000	0.65±0.00	13.9±0.1	0.63±0.01
		$a^*=10$	0.487±0.000	0.86±0.00	14.1±0.1	0.84±0.07
		$a^*=5$	0.309±0.001	0.90±0.01	14.1±0.2	0.90±0.23
		$a^*=2.5$	0.119±0.000	0.61±0.21	14.0±0.5	10.5±6.4
		CF2	⋯	0.87±0.01	13.9±0.0	0.93±0.03
			$-\delta(0)_{xx}^2$			
$-\delta(t)_{xx}^2$	BRC	$a^*=\infty$	0.994±0.001	0.95±0.55	13.4±7.3	
		$a^*=10$	0.623±0.001	1.00±0.00	13.9±0.2	
		$a^*=5$	0.391±0.001	1.01±0.00	14.3±0.1	
		$a^*=2.5$	0.155±0.001	1.05±0.06	14.7±0.5	
	WLC	$a^*=\infty$	0.993±0.001	0.95±0.55	14.0±7.6	
		$a^*=10$	0.630±0.001	1.00±0.00	14.4±0.2	
		$a^*=5$	0.408±0.001	1.01±0.00	14.6±0.2	
		$a^*=2.5$	0.157±0.001	1.04±0.02	14.7±1.0	
(b)						
$\Delta n(t)^*$	BRC	$b^*=10$	0.644±0.000	0.70±0.00	13.3±0.0	2.5±0.0
		$b^*=5$	0.378±0.001	0.70±0.01	13.4±0.1	2.4±0.1
		$b^*=2.5$	0.193±0.000	0.70±0.05	13.6±1.0	2.3±0.5
		CF1	⋯	0.72±0.01	12.7±0.1	2.4±0.0
		RBT	⋯	⋯	13.6	3.5
	WLC	$b^*=10$	0.539±0.001	0.82±0.00	14.1±0.0	0.82±0.03
		$b^*=5$	0.315±0.001	0.85±0.01	14.1±0.2	0.83±0.18
		$b^*=2.5$		0.85±0.01	14.3±0.2	0.87±0.09
		CF1	⋯	0.86±0.05	13.9±0.0	0.95±0.03
		RBT	⋯	⋯	13.9±0.1	4.8±0.6
			$-\delta(0)_{xx}^2$			
$-\delta(t)_{xx}^2$	BRC	$b^*=10$	0.703±0.001	0.93±0.00	13.7±0.1	2.0±0.3
		$b^*=5$	0.433±0.001	0.91±0.02	13.6±0.3	2.5±0.4
		$b^*=2.5$	0.231±0.001	0.87±0.10	14.2±2.0	2.2±1.9
	WLC	$b^*=10$	0.689±0.001	0.99±0.01	14.2±0.2	
		$b^*=5$	0.417±0.001	0.98±0.00	14.1±0.1	
		$b^*=2.5$	0.213±0.001	0.97±0.01	14.3±0.3	

ible model is around three to four times faster for the WLC. These results support the idea that τ_b is mainly related with the internal dynamics of the molecule. In this sense, we remind the reader that we are comparing BRC models with flexibility localized at one flexible joint with WLC models with flexibility uniformly distributed along the molecule. Difference in τ_b are, then, an interesting clue for distinguishing between wormlike and segmental flexibility.

τ_b depends mainly on the type of flexibility but also on the orienting mechanism and for the permanent dipole also on the field intensity. This conclusion is readily obtained from Tables I and II. Except for BRC and induced dipole, an increase in the intensity of the field is matched by a decrease in the value of the faster relaxation time. In our data, this decrease reaches almost 75% when, in the WLC and permanent dipole, the field increases from $a^*=2.5$ to $a^*=\infty$. In all other cases the effect is smaller. This finding is not necessarily against the proposed idea that relaxation times are char-

Downloaded 05 Apr 2005 to 155.54.98.94. Redistribution subject to AIP license or copyright, see http://jcp.aip.org/jcp/copyright.jsp

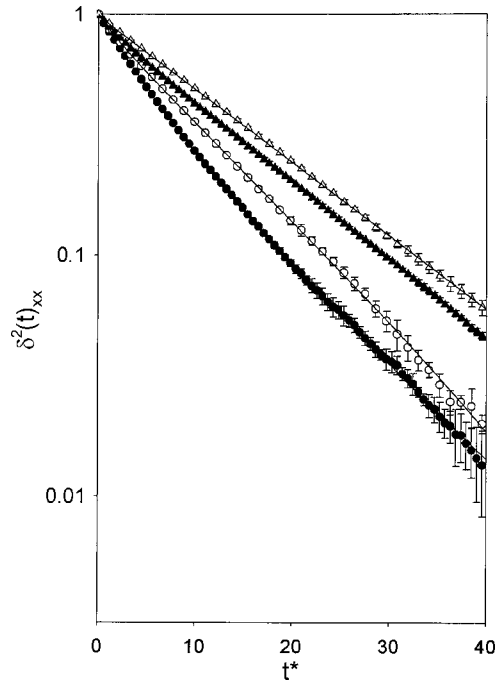

FIG. 2. Evolution of $\delta(t)^2_{xx}$ when electric field has been removed. Induced dipole, $b^*=10$. Legend: black circles, BRC with $\langle s(\infty)^2\rangle/s^2_{str}=0.62$; white circles, WLC with $\langle s(\infty)^2\rangle/s^2_{str}=0.62$; black triangles, BRC with $\langle s(\infty)^2\rangle/s^2_{str}=0.77$; white triangles, WLC with $\langle s(\infty)^2\rangle/s^2_{str}=0.77$.

acteristics of a molecule and do not depend on the method used to obtain them.[42] We remind the reader that τ_b is a

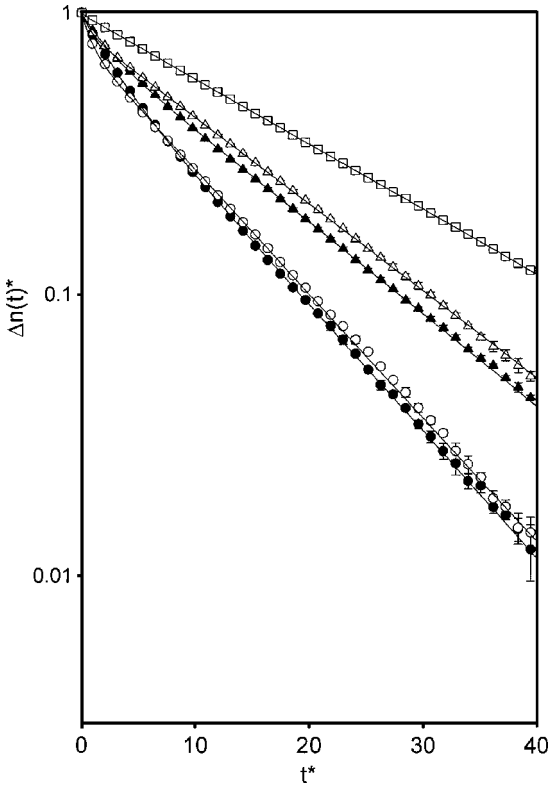

FIG. 3. Birefringence decay profiles for different degrees of flexibility. Permanent dipole, $a^*=10$. Legend: black circles, BRC with $\langle s(\infty)^2\rangle/s^2_{str}=0.62$; white triangles, WLC with $\langle s(\infty)^2\rangle/s^2_{str}=0.62$; black triangles, BRC with $\langle s(\infty)^2\rangle/s^2_{str}=0.77$; white triangles, WLC with $\langle s(\infty)^2\rangle/s^2_{str}=0.77$; white squares, quasirigid model with $\langle s(\infty)^2\rangle/s^2_{str}=0.97$.

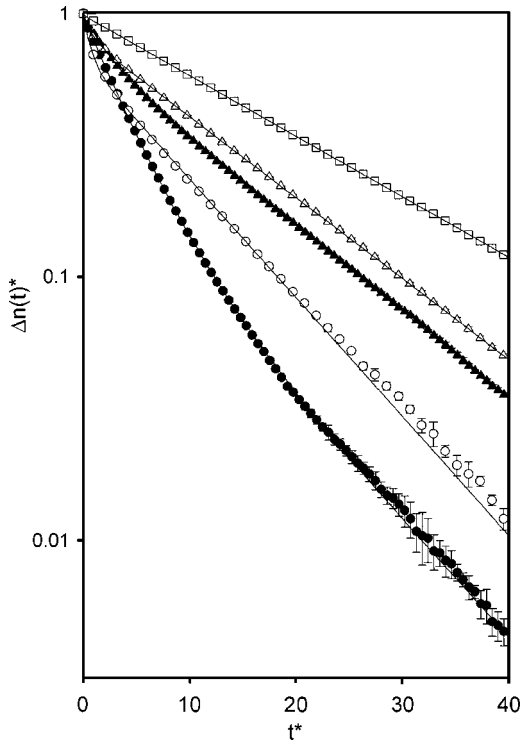

FIG. 4. Birefringence decay profiles for different degrees of flexibility. Induced dipole, $b^*=10$. Legend: black circles, BRC with $\langle s(\infty)^2\rangle/s^2_{str}=0.62$; white circles, WLC with $\langle s(\infty)^2\rangle/s^2_{str}=0.62$; black triangles, BRC with $\langle s(\infty)^2\rangle/s^2_{\mathbf{str}}=0.77$; white triangles, WLC with $\langle s(\infty)^2\rangle/s^2_{str}=0.77$; white squares, quasirigid model with $\langle s(\infty)^2\rangle/s^2_{str}=0.97$.

certain average of the faster relaxation times and their amplitudes. The practical consequence of the described dependence is that a proper analysis of τ_b should include values at different field intensities.

In the WLC model, differences in the decay profile are significant between orienting mechanisms and field intensity, at high flexibility values. When flexibility is low, the decay curves depend very little on the orienting mechanism or the field intensity. τ_b is very similar for all the curves of WLC, independently of flexibility, orienting mechanism, or field intensity. Differences in the values of the amplitudes, although small, are more easily detectable when flexibility is high, especially for the induced dipole model.

Differences in the decay curves between BDEF and BDCF are small. This conclusion is very interesting because it extends the application range of the BDCF procedure. The benefit is that this method is computationally faster that the BDEF, although possible dependences on the intensity of the field, which could be detected with data of high statistical quality, cannot be found.

The values obtained with the RBT for τ_1 are usually very close to those of BDEF. Differences depend on the type of flexibility, orienting mechanism, and intensity of the field. The maximum difference ($\approx$15%) appears in the BRC model with high flexibility. When the orienting mechanism is the permanent dipole and the field intensity is low the coincidence is nearly perfect, within the standard deviation. As a consequence, in a good number of cases, the RBT could be a reasonable approximation for τ_1. This result agrees with the

Downloaded 05 Apr 2005 to 155.54.98.94. Redistribution subject to AIP license or copyright, see http://jcp.aip.org/jcp/copyright.jsp

idea that the longest relaxation time depends mainly on the overall dimensions of the molecule.

Values of τ_b are totally different for RBT and BDEF. These results again support the idea that the faster relaxation time is mainly related with the internal dynamics of the molecule and reflects the effects of rigidity versus flexibility. One consequence is that, in the case of the quasirigid model, both treatments give essentially a single relaxation time.

The longest relaxation times for $\delta(t)^2_{xx}$ are slightly higher than those of $\Delta n(t)^*$. In addition, for the WLC model the curve is clearly monoexponential in all the cases studied. The same can be observed for the BRC model and the permanent dipole orientation system although, when the type of dipole is induced, a second exponential can be detected.

There is less deformation and faster recovery in the WLC model under the influence of the same field for the permanent dipole orienting mechanism. We have studied through $\delta(t)^2$ [Eq. (12)] the time course of the deformation (results not shown). In the case of the BRC model, for the same intensity of the field and $\langle s(\infty)^2\rangle/s^2_{str}$, the increase in $\delta(t)^2$ roughly doubles that of the WLC model. At the same time the recovery is slower in the BRC model by a factor of 2–3. This is another manifestation of the way in which flexibility is distributed in the two different cases.

Interpretation of experimental results

Although the objective of this work was not the interpretation of any specific experimental results, some interesting consequences can be observed from our results when trying to analyze experiments. One of these is that dynamic electric field scattering experiments are a source of information which can be treated in coordination with birefringence experiments. Another is that we must remember that if the longest relaxation time is the only parameter obtained from the experiments, we shall lose critical information, concerning both the conformation and the dynamics, which can be obtained from TEB. Furthermore, the longest relaxation time can be interpreted in terms of the radius of gyration, independently of the model we use for the flexibility and the orientation mechanism; in other words, very little information about the type of flexibility or orientation mechanism can be obtained if τ_1 is the only parameter used. If the experimental results are of sufficient statistical quality, then attention must be paid to the possible dependence of the intensity of the field. If this is not the case, results from the RBT could be sufficient for a proper interpretation of the longest relaxation time and those from BDCF for that of the whole decay profile.

ACKNOWLEDGMENTS

This work was funded by Grant No. BQU2003-04517 from Dirección General de Investigación (Ministerio de Ciencia y Tecnología). H.E.P. was supported by a predoctoral FPU fellowship from Ministerio de Educación y Ciencia.

[1]E. Frederick and C. Houssier, *Electric Dichroism and Electric Birefringence* (Clarendon, Oxford, 1973).
[2]*Molecular Electro-Optic Properties of Macromolecules and Colloid in Solution*, edited by S. Krause (Plenum, New York, 1981).
[3]E. Riande and E. Saiz, *Dipole Moments and Birefringence of Polymers* (Prentice Hall, Englewoods Cliffs, New Jersey, 1992).
[4]P. J. Hagerman, Curr. Opin. Struct. Biol. **6**, 643 (1996).
[5]P. J. Hagerman, Methods Enzymol. **317**, 440 (2000).
[6]Y. Lu, B. Weers, and N. C. Stellwagen, Biopolymers **61**, 261 (2002).
[7]T. Grycuk, J. Antosiewicz, and D. Porschke, J. Phys. Chem. **98**, 10881 (1994).
[8]M. Fixman and S. Jagannathan, J. Chem. Phys. **75**, 4048 (1981).
[9]D. C. Rau and E. Charney, Biophys. Chem. **14**, 1 (1982).
[10]D. C. Rau and E. Charney, Macromolecules **16**, 1653 (1983).
[11]T. Bellini, V. Degiorgio, and F. Mantegazza, Colloids Surf., A **140**, 103 (1998).
[12]R. J. Lewis, S. A. Allison, D. Eden, and R. Pecora, J. Chem. Phys. **89**, 2490 (1988).
[13]S. Dieckman, W. Hillen, B. Morgener, R. D. Wells, and D. Porschke, Biophys. Chem. **15**, 263 (1982).
[14]M. Hogan, N. Dattagupta, and D. M. Crothers, Proc. Natl. Acad. Sci. U.S.A. **75**, 195 (1978).
[15]N. C. Stellwagen, Biopolymers **20**, 399 (1981).
[16]J. G. Elias and D. Eden, Macromolecules **14**, 410 (1981).
[17]S. A. Allison and P. Nambi, Macromolecules **25**, 759 (1992).
[18]M. Zacharias and P. J. Hagerman, Biophys. J. **73**, 318 (1997).
[19]P. J. Heath, S. A. Allison, J. A. Gebe, and J. M. Schurr, Macromolecules **28**, 6600 (1995).
[20]B. Carrasco, F. G. Díaz, M. C. López Martínez, and J. García de la Torre, J. Phys. Chem. **103**, 7822 (1999).
[21]F. G. Díaz, B. Carrasco, M. C. López Martínez, and J. García de la Torre, J. Phys. Chem. **104**, 12339 (2000).
[22]H. E. Pérez Sánchez, J. García de la Torre, and F. G. Díaz Baños, J. Phys. Chem. **106**, 6754 (2002).
[23]H. E. Pérez Sánchez, J. García de la Torre, and F. G. Díaz Baños, J. Phys. Chem. **107**, 13192 (2003).
[24]J. E. Hearst, J. Chem. Phys. **38**, 1062 (1963).
[25]P. Hagerman and B. H. Zimm, Biopolymers **20**, 1481 (1981).
[26]J. J. García Molina, M. C. López Martínez, and J. García de la Torre, Biopolymers **29**, 883 (1990).
[27]J. García de la Torre, in *Molecular Electro-Optics*, Rotational diffusion coefficients, edited by S. Krause (Plenum, New York, 1981), pp. 75–103.
[28]J. García de la Torre, Eur. Biophys. J. **23**, 307 (1994).
[29]J. García de la Torre and V. A. Bloomfield, Biopolymers **16**, 1747 (1977).
[30]J. García de la Torre, S. Navarro, M. C. López Martínez, F. G. Díaz, and J. J. López Cascales, Biophys. J. **67**, 530 (1994).
[31]J. García de la Torre and V. A. Bloomfield, Q. Rev. Biophys. **14**, 81 (1981).
[32]W. A. Wegener, J. Chem. Phys. **76**, 6425 (1982).
[33]W. A. Wegener, Biopolymers **25**, 627 (1986).
[34]W. A. Wegener, R. M. Dowben, and V. J. Koester, J. Chem. Phys. **70**, 622 (1979).
[35]W. A. Wegener, R. M. Dowben, and V. J. Koester, J. Chem. Phys. **73**, 4086 (1980).
[36]J. García de la Torre, P. Mellado, and V. Rodes, Biopolymers **24**, 2145 (1985).
[37]S. C. Harvey, J. Chem. Phys. **69**, 3426 (1978).
[38]S. C. Harvey, Biopolymers **18**, 1081 (1979).
[39]S. C. Harvey, P. Mellado, and J. García de la Torre, J. Chem. Phys. **78**, 2081 (1983).
[40]P. Mellado, A. Iniesta, F. G. Díaz, and J. García de la Torre, Biopolymers **27**, 1771 (1988).
[41]D. B. Roitman and B. H. Zimm, J. Chem. Phys. **81**, 6356 (1984).
[42]D. B. Roitman and B. H. Zimm, J. Chem. Phys. **81**, 6348 (1984).
[43]A. Iniesta, F. G. Díaz, and J. García de la Torre, Biophys. J. **54**, 269 (1988).
[44]E. Vacano and P. J. Hagerman, Biophys. J. **73**, 306 (1997).
[45]A. Frazer-Abel and P. J. Hagerman, J. Mol. Biol. **285**, 581 (1999).
[46]M. W. Friedrich, E. Vacano, and P. J. Hagerman, Proc. Natl. Acad. Sci. U.S.A. **95**, 3572 (1998).
[47]J. B. Mills, E. Vacano, and P. J. Hagerman, J. Mol. Biol. **285**, 245 (1999).
[48]J. W. Orr, P. J. Hagerman, and J. R. Williamson, J. Mol. Biol. **275**, 453 (1998).
[49]B. Carrasco, A. Pérez Belmonte, M. C. López Martínez, and J. García de la Torre, J. Chem. Phys. **100**, 9900 (1996).

Downloaded 05 Apr 2005 to 155.54.98.94. Redistribution subject to AIP license or copyright, see http://jcp.aip.org/jcp/copyright.jsp

[50]S. Navarro, B. Carrasco, M. C. López Martínez, and J. García de la Torre, J. Polym. Sci., Part B: Polym. Phys. **35**, 689 (1997).
[51]A. Pérez Belmonte, M. C. López Martínez, and J. García de la Torre, J. Chem. Phys. **95**, 952 (1991).
[52]A. Pérez Belmonte, M. C. López Martínez, and J. García de la Torre, J. Chem. Phys. **95**, 5661 (1991).
[53]P. Hagerman, Biopolymers **20**, 1503 (1981).
[54]J. A. Bertolotto, M. G. Campo, G. B. Roston, and M. E. Ascheri, Colloids Surf., A **203**, 167 (2002).
[55]P. J. Hagerman, Annu. Rev. Biophys. Biomol. Struct. **26**, 139 (1997).
[56]Y. Lu, B. Weers, and N. C. Stellwagen, Biopolymers **70**, 270 (2003).
[57]M. W. Friedrich, F. U. Gast, E. Vacano, and P. J. Hagerman, Proc. Natl. Acad. Sci. U.S.A. **92**, 4803 (1995).
[58]F. G. Díaz and J. García de la Torre, J. Chem. Phys. **88**, 7698 (1988).
[59]*Modern Theory of Polymer Solutions*, edited by H. Yamakawa (Harper and Row, New York, 1971).
[60]F. G. Díaz, J. J. Freire, and J. García de la Torre, Macromolecules **23**, 3144 (1990).
[61]F. G. Díaz and J. García de la Torre, Macromolecules **27**, 5371 (1994).
[62]F. G. Díaz, A. Iniesta, and J. García de la Torre, Biopolymers **29**, 547 (1990).
[63]F. G. Díaz, J. J. López Cascales, and J. García de la Torre, J. Biochem. Biophys. Methods **26**, 261 (1993).
[64]A. Iniesta, M. C. López Martínez, and J. García de la Torre, J. Fluoresc. **1**, 129 (1991).
[65]D. L. Ermak and J. A. McCammon, J. Chem. Phys. **69**, 1352 (1978).
[66]A. Iniesta and J. García de la Torre, J. Chem. Phys. **92**, 2015 (1990).
[67]J. Rotne and S. Prager, J. Chem. Phys. **50**, 4831 (1969).
[68]H. Yamakawa, J. Chem. Phys. **53**, 436 (1970).
[69]J. García de la Torre, H. E. Pérez Sánchez, A. Ortega, J. G. Hernández Cifre, M. X. Fernandes, F. G. Díaz Baños, and M. C. López Martínez, Eur. Biophys. J. **32**, 477 (2003).
[70]SIGMAPLOT for Windows, Version 7.00, 2001.
[71]J. J. López Cascales, S. Navarro, and J. García de la Torre, Macromolecules **25**, 3574 (1992).
[72]B. R. Jennings, in *Molecular Electro-optics*, Light scattering in electric fields, edited by S. Krause (Plenum, New York, 1981).
[73]G. Khanarian and R. S. Stein, Macromolecules **20**, 2858 (1987).
[74]J. J. García Molina and J. García de la Torre, Int. J. Biol. Macromol. **6**, 170 (1984).

Downloaded 05 Apr 2005 to 155.54.98.94. Redistribution subject to AIP license or copyright, see http://jcp.aip.org/jcp/copyright.jsp